Journal of Chromatography, 391 (1987) 296–302
Elsevier Science Publishers B.V., Amsterdam — Printed in The Netherlands

CHROM. 19 297

Note

Direct coupling of micro high-performance liquid chromatography with fast atom bombardment mass spectrometry

III. Application to oligosaccharides

YUKIO ITO, TOYOHIDE TAKEUCHI and DAIDO ISHII*
Department of Applied Chemistry, Faculty of Engineering, Nagoya University, Chikusa-ku, Nagoya-shi, 464 (Japan)
MASASHI GOTO
Research Center for Resource and Energy Conservation, Nagoya University, Chikusa-ku, Nagoya-shi, 464 (Japan)
and
TOKUO MIZUNO
Analytical Instruments Technical and Engineering Division JEOL Ltd., 1418 Nakagami, Akishima-shi, 196 (Japan)
(First received July 29th, 1986; revised manuscript received November 11th, 1986)

The analysis of saccharides is very important in various fields such as chemistry, biology, pharmacy, medicine and food industry. Chromatographic methods presently used involve gas chromatography–mass spectrometry (GC–MS)[1], high-performance liquid chromatography (HPLC)[2] and off-line HPLC–fast atom bombardment mass spectrometry (FABMS)[3]. Suitable derivatization of saccharides is necessary for GC analysis owing to their high polarities and low volatilities, while they are derivatized to improve detectability in HPLC. FABMS and secondary-ion mass spectrometry (SIMS) are especially suitable for the analysis of high-molecular-weight, polar or thermally labile compounds[4], which can be separated by HPLC. Some methods have been developed for coupling of HPLC with FABMS[5] and of thin-layer chromatography with SIMS[6,7]. We have developed an on-line interface for micro HPLC–FABMS[8,9]. This system was successfully applied to the analysis of oligosaccharides.

EXPERIMENTAL

Micro HPLC–FABMS system

Details of the interface and the system have been described[8,9]. The HPLC system was assembled using a Micro Feeder MF-2 pump (Azumadenkikogyo, Tokyo, Japan) equipped with a gas-tight syringe MS-GAN 050 (0.5 ml; Ito Seisakusho, Tokyo, Japan), a line filter (3-μm element), a valve injector (0.02 μl; Jasco, Tokyo, Japan), a home-made separation column and a GC oven. The separation column was made from fused-silica tubing (150 mm × 0.26 mm I.D. or 200 mm × 0.22 mm I.D.), packed with SZ-5532 (6 μm; Showadenko, Tokyo, Japan) by the method described[10].

0021-9673/87/$03.50 © 1987 Elsevier Science Publishers B.V.

Glycerol–acetonitrile–water–methanol (10:63:18:9) was used as a mobile phase, and the flow-rate was 1.04 μl/min. Glycerol acts as the matrix for FAB ionization, and methanol is added to increase the solubility of glycerol in the mobile phase. The column was placed in the GC oven and the temperature was kept at 60°C to avoid separation of anomers of saccharides. The separation conditions were monitored with a UVIDEC-100V UV spectrophotometer (Jasco) at 197 nm, in the absence of glycerol.

Mass spectrometer

A JMS-DX300 double-focusing mass spectrometer (JEOL, Tokyo, Japan) was employed with a liquid nitrogen trap. Xenon atoms with energy 5 keV were used for ionization. The scan range was set at m/z 150–1000 and the temperature of the ion-source chamber was 130°C.

All the solvents and samples were obtained from Wako (Osaka, Japan).

RESULTS AND DISCUSSION

Fig. 1 illustrates the ionization process for our system, in which glycerol is contained in the mobile phase. The organic solvents and water in the column effluent are immediately vaporized on the surface of the frit, while the solute and glycerol are

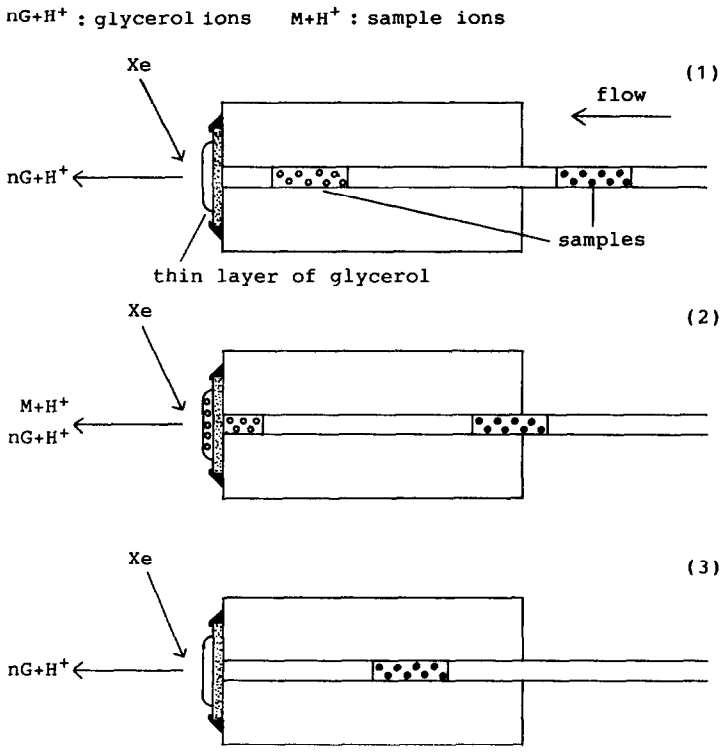

Fig. 1. Ionization process.

left on the surface and are bombarded by the xenon beam. The supply rate of glycerol depends on its concentration in the mobile phase and the flow-rate. On the other hand, the vaporization rate is dependent on the sputtering efficiency, degree of evacuation, the chamber temperature, the surface area of the glycerol layer, etc. The supply rate and vaporiation rate of glycerol could be made to coincide by controlling the parameters mentioned above. Consequently, the amount of glycerol on the frit surface can be kept constant, leading to stable FAB ionization. The thickness of the glycerol layer may be very thin, because when the flow of the mobile phase is stopped the ions based on glycerol almost disappear in about 2 s.

The reproducibility of ionization was examined by repeated injection of maltohexaose (MW 990), as shown in Fig. 2. In this case, the interface was directly connected to the sample injector without the separation column. The sample was dissolved in distilled water containing 10% glycerol, and a 0.02-μl solution containing 1 nmol of maltohexaose was injected. The signal at m/z = 461 in the mass chromatograms corresponds to the protonated pentamer of glycerol, which shows stable ionization. The signal intensity at m/z = 325 was three times stronger than that at m/z = 991, but the signal-to-noise (S/N) ratio was much worse since the background signal of glycerol was strong at masses below m/z = 400 (Fig. 3B). The peak shape and S/N ratio of the signal reconstructed from m/z = 990 to 992 were better than those for m/z = 991. From these observations it was concluded that the reconstructed signal was the most suitable for quantitative analysis of maltohexaose.

The peak width at the half peak height of maltohexaose is much wider than that of bile acids[9], because the former compounds is more difficult to ionize than the latter. It is necessary to ionize the sample more efficiently. The peak profiles had a reproducibility of 11% relative standard deviation, a good symmetry and little tailing, indicating that the samples introduced into the interface were completely consumed and did not remained on the surface of the frit. The detection limit was 0.1 nmol (S/N = 2) with this flow-injection system.

Fig. 3 shows the mass spectra of maltohexaose. The top trace (A) and the middle trace (B) correspond to the peak and the background, respectively. The bot-

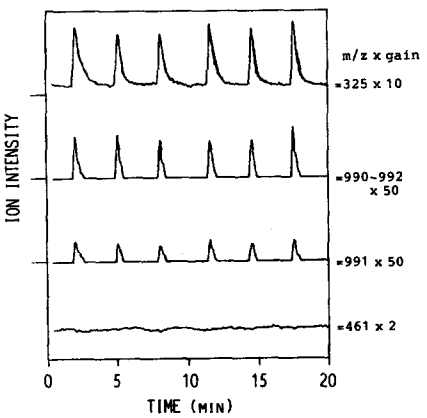

Fig. 2. Ion monitoring of glycerol and maltohexaose. Mobile phase: glycerol–acetonitrile–water–methanol (10:63:18:9). Flow-rate: 1.04 μl/min. Sample: 1 nmol of maltohexaose.

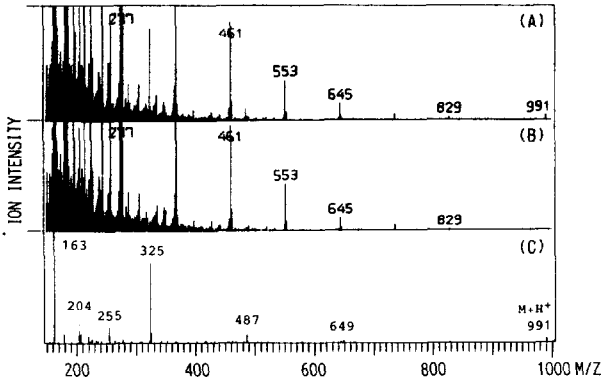

Fig. 3. Mass spectra of maltohexaose. (A) Spectrum at the peak in the mass chromatogram; (B) spectrum at the valley in the mass chromatogram; (C) difference spectrum, (A − B). Operating conditions as in Fig. 2.

tom trace (C) represents the difference spectrum (A − B), in which the background due to the matrix is removed. The signal at m/z = 991 corresponds to $(M + H)^+$, while those at m/z = 649, 487, 325 and 163 are due to fragment ions. An amount of 0.5 nmol was necessary to obtain a good mass spectrum.

Fig. 4 shows mass chromatograms of a standard mixture of glucose (MW 180), lactose (MW 342) and raffinose (MW 504). The samples were dissolved in distilled water, and 80 ng of each saccharide were injected. The signals at m/z = 461, 273, 343 and 505 corresponds to the protonated pentamer of glycerol, $(M + \text{glycerol} + H)^+$ of glucose, $(M + H)^+$ of lactose and of raffinose, respectively.

Fig. 5 shows mass chromatograms of a mixture of glucose, maltotriose (MW

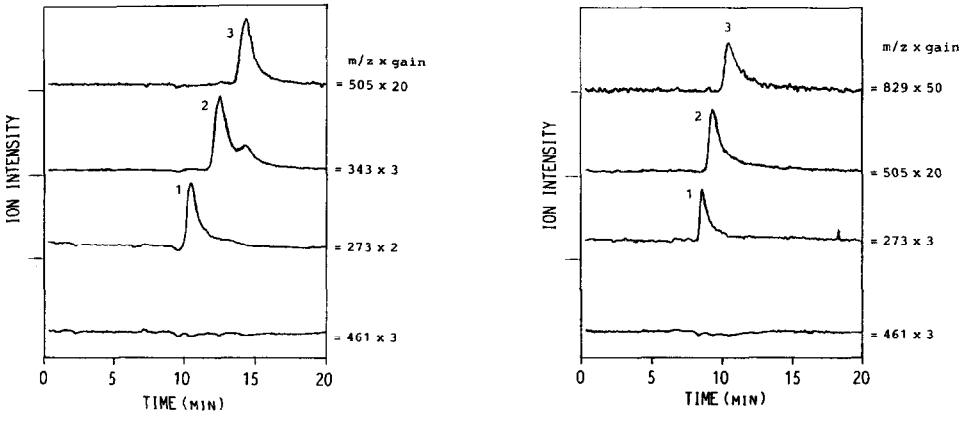

Fig. 4. Separation of standard oligosaccharides (I). Column: SZ-5532 (6 μm), 150 mm × 0.26 mm I.D. Column temperature: 60°C. Mobile phase as in Fig. 1. Sample: 800 ng each of glucose (1), lactose (2) and raffinose (3).

Fig. 5. Separation of standard oligosaccharides (II). Conditions as in Fig. 4 except column 200 mm × 0.22 mm I.D. Sample: 2 nmol each of glucose (1), maltotriose (2) and maltopentaose (3).

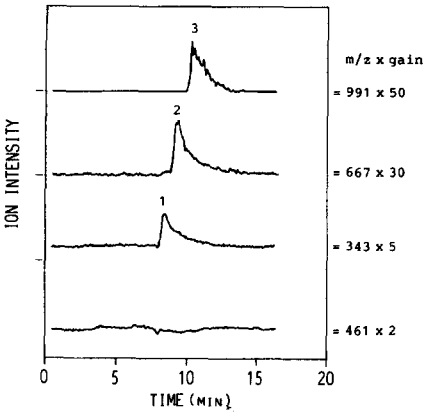

Fig. 6. Separation of standard oligosaccharides (III). Operating conditions as in Fig. 5. Sample: 2 nmol each of maltose (1), maltotetraose (2) and maltohexaose (3).

504) and maltopentaose (MW 828), and Fig. 6 those of maltose (MW 342), maltotetraose (MW 666) and maltohexaose (MW 990). A 2-nmol amount of each sample was injected. The protonated molecular ions were monitored except for glucose. Stable ionization and high sensitivity of detection were obtained. The detection limit of maltohexaose in the mass chromatogram was 0.3 nmol (S/N = 2) and 1 nmol was necessary to obtain a good mass spectrum. The plugging problem due to the laeked packing materials and/or dusts in the eluent has not been encountered in this work. The peak width observed for FABMS detection was two or three times greater than

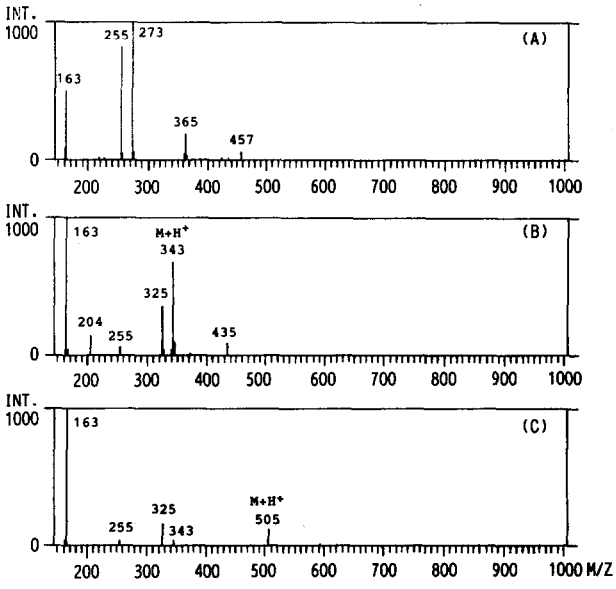

Fig. 7.

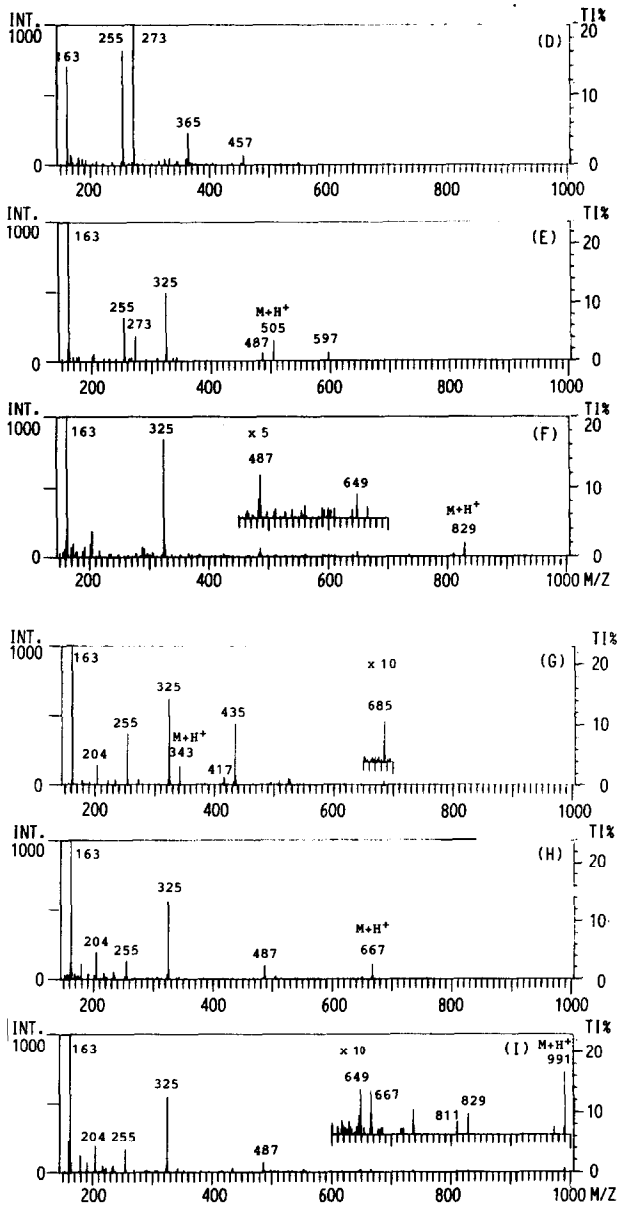

Fig. 7. Difference mass spectra of oligosaccharides. (A) Glucose, (B) lactose, (C) raffinose in Fig. 4; (D) glucose, (E) maltotriose, (F) maltopentaose in Fig. 5; (G) maltose, (H) maltotetraose, (I) maltohexaose in Fig. 6.

that observed for UV detection, and the degree of peak tailing was greater. These problems may be improved by considering the structure of the interface, *e.g.*, the pore size, the material and the thickness of the frit. The baseline at m/z = 829 in Fig. 5 is noisy, because this mass number is the same as that of the protonated nanomer of glycerol.

Fig. 7 shows the difference spectra of all the saccharides in Figs. 4–6. These spectra show a protonated molecular ion and fragment ions due to cleavage of the glycoside bond, which reflect the structures of the saccharides.

REFERENCES

1 I. Brondz and I. Olsen, *J. Chromatogr.*, 310 (1984) 261.
2 F. M. Eggert and M. Jones, *J. Chromatogr.*, 333 (1985) 123.
3 M. Arita, M. Iwamori, T. Higuchi and Y. Nagai, *J. Biochem. (Tokyo)*, 95 (1984) 971.
4 K. Harada, M. Suzuki and H. Kambara, *Org. Mass Spectrom.*, 13 (1982) 386.
5 J. G. Stroh, J. C. Cook, R. M. Milberg, L. Brayton, T. Kihara, Z. Huang, K. L. Rinehart, Jr. and I. A. S. Lewis, *Anal. Chem.*, 57 (1985) 985.
6 T. T. Chang, J. O. Lay and R. J. Francel, *Anal. Chem.*, 56 (1984) 109.
7 Y. Kushi and S. Handa, *J. Biochem (Tokyo)*, 98 (1985) 265.
8 Y. Ito, T. Takeuchi, D. Ishii and M. Goto, *J. Chromatogr.*, 346 (1985) 161.
9 Y. Ito, T. Takeuchi, D. Ishii, M. Goto and T. Mizuno, *J. Chromatogr.*, 358 (1986) 201.
10 T. Takeuchi and D. Ishii, *J. Chromatogr.*, 213 (1981) 25.